LBL-35811
UC-414
Preprint

Lawrence Berkeley Laboratory
UNIVERSITY OF CALIFORNIA

Physics Division

Submitted to Japanese Journal of Applied Physics

Improved Electronic Transport Characteristics of Amorphous Silicon by Hydrogen Dilution of Silane

A. Mireshghi, W.S. Hong, J. Drewery, T. Jing, S.N. Kaplan,
H.K. Lee, and V. Perez-Mendez

July 1994

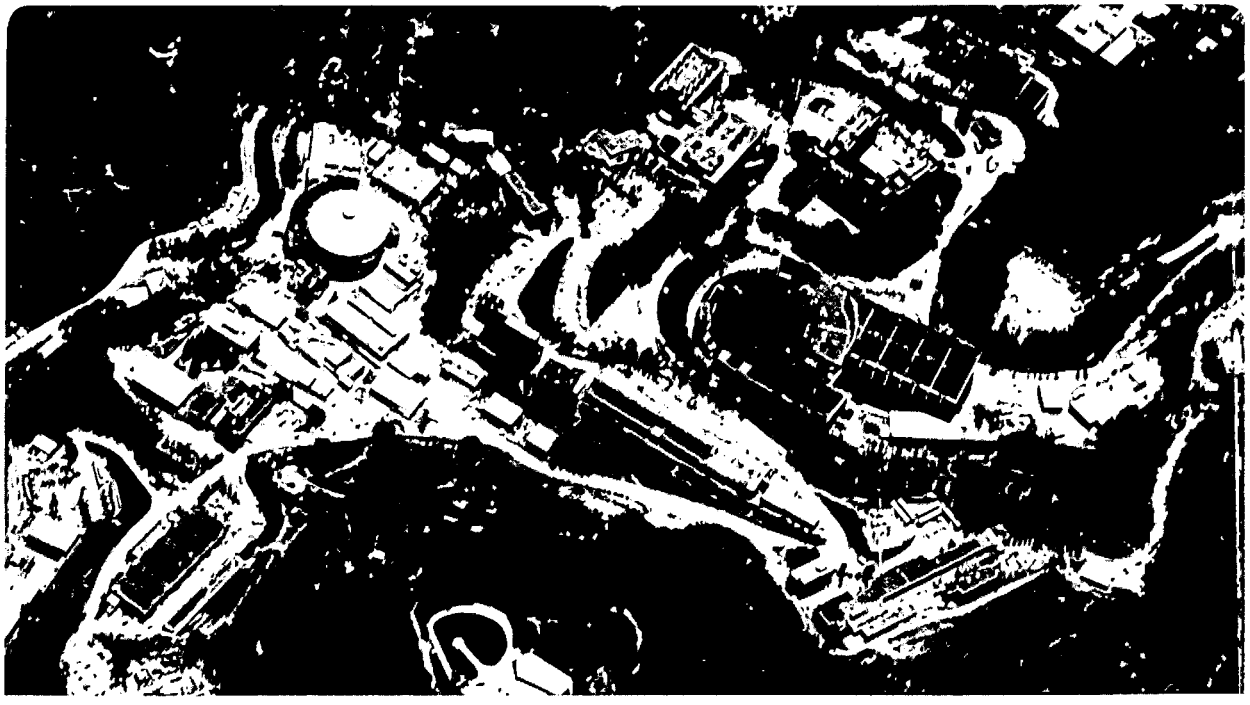

Prepared for the U.S. Department of Energy under Contract Number DE-AC03-76SF00098

DISCLAIMER

Sent for Publication in: Jpn.J.Appl. Phys. 1994

LBL-35811

IMPROVED ELECTRONIC TRANSPORT CHARACTERISTICS OF AMORPHOUS SILICON BY HYDROGEN DILUTION OF SILANE

A. Mireshghi, W.S. Hong, J. Drewery, T. Jing, S.N. Kaplan, H.K. Lee
and V. Perez-Mendez

Physics Division
Lawrence Berkeley Laboratory*
University of California
Berkeley, CA 94720

JULY 1994

---

*This work was supported by the Director, Office of Energy Research, Office of High energy Nuclear Physics, High Energy Physics Division of U.S. Department of Energy under Contract Number DE-AC03-76SF00098

Sent for Publication in: Jpn.J.Appl. Phys. 1994

Improvement of Electronic Transport Characteristics of Amorphous Silicon By Hydrogen Dilution of Silane

A. Mireshghi*, W.S. Hong, J. Drewery, T. Jing, S. N. Kaplan,
H. K. Lee and V. Perez-Mendez,

Lawrence Berkeley Laboratory, University of California, Berkeley, CA 94720

We have investigated the electrical and material properties of intrinsic amorphous silicon deposited with hydrogen dilution of silane. The hydrogenated material was used as intrinsic layers of n-i-p diodes, which showed interesting electrical characteristics which have not been reported before. From time of flight (TOF) measurement for our best samples we obtained mobility (μ) values about 3-4 times larger than our standard amorphous silicon (a-Si:H). Approximately a factor of 2 improvement was observed for $\mu\tau$ values. The N_D^* values derived from hole-onset measurements show lower ionized dangling bond density than the normal a-Si:H material. At a hydrogen to silane gas flow ratio of 20, some microcrystalline formation was observed in the deposited material. We propose a simple macroscopic model to assess the effect of microcrystals and grain boundaries on the electronic properties of mixed amorphous and microcrystalline material.

KEYWORDS: amorphous silicon, hydrogen dilution, microcrystalline silicon, electronic transport properties, PE-CVD deposition conditions, TOF measurement, defect density, mobility, lifetime, $\mu\tau$–value

---

* On leave from Sharif University of Technology, Tehran, Iran

1. Introduction

Hydrogen dilution of silane has been widely used to produce microcrystalline silicon, specially by plasma enhanced chemical vapor deposition (PECVD) technique.[1] This material doped with Boron, has been considered as window layers of solar cells.[2-4], due to its low optical absorption and high electrical conductivity compared to hydrogenated amorphous silicon (a-Si:H). In addition, intrinsic and n^+-doped microcrystalline silicon has been used as channel, source and drain contact material in thin film transistors (TFT). The channel mobility of these devices is reported to be ~ 6.5 cm^2/Vs, which is a factor of 5 higher than that of a-Si:H thin film transistors.[5]

The objective of the present work was to study the effect of excess hydrogenation of silane on the electronic transport properties of PECVD deposited films, which are of interest in radiation detection applications. Our group, as well as others, have successfully used a-Si:H in the form of n-i-p diode structures to detect charged particles, X-rays, gamma rays, and neutrons.[6-9] For radiation detection applications, an important characteristic is the mobility lifetime product ($\mu\tau$) value. This parameter determines the mean free path of charge carriers ($d= \mu\tau E$) within the intrinsic layer, which in turn controls the charge collection efficiency of the detector. The existing data on electronic properties of microcrystalline silicon, mostly deal with dark and photo conductivity and bandgap measurement,[10-12] and direct measurement results on electronic transport properties such as carrier mobility and lifetime, especially for undoped μc-Si layers are not available. Our initial assumption was that by using hydrogen dilution of silane we would produce amorphous silicon enriched with a microcrystalline phase, which would have higher mobility than normal a-Si:H. But we were not certain about the $\mu\tau$ value, and especially we were concerned with charge carrier trapping by the crystallite grain boundaries. Our investigations show that the quality of a-Si:H material was indeed improved by using hydrogen dilution of silane; however the conclusion was that the improvements were not directly related to microcrystal formation, but rather were the result of hydrogen effect on the amorphous part .[13]

In this paper, we will present new measurement results which further confirm our previous conclusion, and also describe a macroscopic model which is capable of providing a simple, but meaningful picture of the effect of microcrystalline and grain boundaries on electronic transport of mixed amorphous-microcrystalline materials.

2. Sample Preparation and Structure

Our measured samples were 5-8 μm thick n-i-p diodes, deposited in our PECVD facility at an RF frequency of 85 MHz. For substrates we used Corning 7059 glass, and the top and bottom contacts were sputtered transparent Cr layers. The 300 nm thick n and p doped layers were deposited under our standard a-Si:H deposition conditions. The hydrogen dilution was only used

Table I. Deposition conditions for the intrinsic layers of various runs

Run No.	[H2] /[SiH4]	T_S (o C)	PD (mW /cm ^{2})	Dep. Rate (A°/sec)
MC388	10	190	60	2.8
MC392	10	190	90	4.1
MC389	10	250	60	3.7
MC361	15	190	60	4
MC362	15	190	90	4.3
MC363	15	250	60	3
MC292	20	190	60	2.2
MC370	20	190	90	2.1
MC354	20	250	60	2.2

for the intrinsic layers. The deposition conditions for these layers are given in Table I. The sum of H_2 and SiH_4 flow rates were kept constant at 100 sccm, while the flow rate ratios (hereafter referred to as: hydrogen ratio) were varied for different samples. All the successful samples were deposited at a pressure of 1 Torr. Deposition rates of our various samples versus hydrogen ratio are shown in Fig. 1. In the legend of this figure, T1 and T2 are used to denote T_S of 190 °C and 250 °C. Also, P1 and P2 represent the RF power of 60 and 90 mW/cm^2, respectively. The same notations are used in Figs. 2-6, 9. As seen, the use of higher power resulted in larger deposition rates, except for the hydrogen ratio of 20, where the rate is not sensitive to temperature and power variation. At the T_S =250 °C, the deposition rate decreases with increasing hydrogen dilution. In general the deposition rates are about a half to one third of that of the standard a-Si:H at this RF frequency (85 MHz).

3. Measurements

3.1 *Electronic transport parameters*

The electron and hole mobilities were measured using the standard time of flight technique (TOF), by illuminating the p and n sides respectively. In our TOF experimental setup, we use a 3 ns (FWHM) Nitrogen_Dye laser to produce 510 nm light (MFP~0.2 μm in a-Si:H) The laser is triggered externally by a pulse from a high voltage pulser. For transient photo-current measurement, the trigger pulse is delayed so that laser fires 50-100 μs after the start of the applied

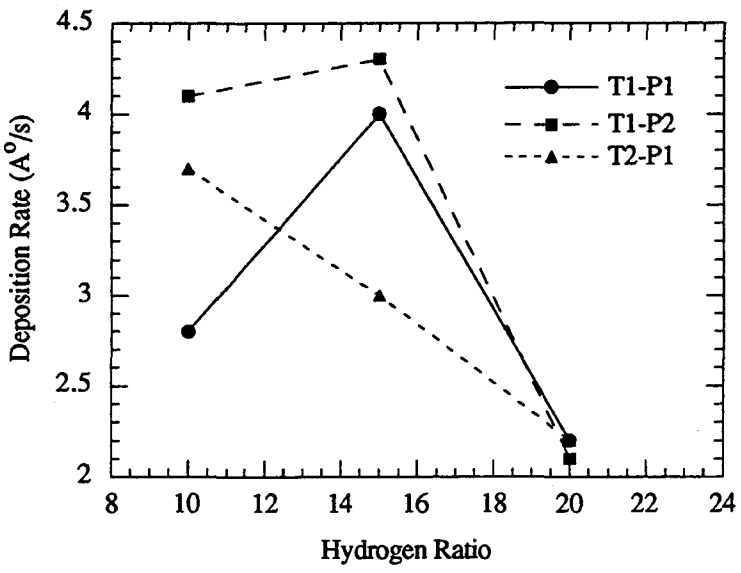

Fig. 1 Variation of deposition rate with hydrogen ratio for 3 different deposition conditions; T1 and T2 refer to T_S of 190 and 250 °C, P1 and P2 refer to RF powers of 60 and 90 mW/cm^2.

bias. The purpose of pulsing the bias was to provide a uniform electric field across the i layer. To find the mobility for each sample, we measured transient times (T_t) at several bias voltages and plotted the measured values versus applied bias. The data were then fitted to:

$$T_t = T_0 + \frac{d^2}{(V_0 + V)\mu_a} \tag{1}$$

where, T_t , d, μ, V_a, V_0 are the transit time, thickness of the intrinsic layer, mobility, applied bias, and the built in potential, respectively. The thicknesses of the i layers were found from profilameter measurement of the n-i-p samples. Figures 2 and 3, show the results of electron and hole mobility measurements vs. hydrogen ratio for 3 sets of deposition condition. The mobilities peak at a hydrogen ratio of 15, for both electrons and holes, except for the samples deposited at T_S =250 °C, for which the mobility drops with increasing hydrogen dilution. The samples deposited at T_S =190 °C and P=60 mW/cm^2, show the highest electron and hole mobilities, a factor of about 4 and 3 higher than the respective normal a-Si:H values.

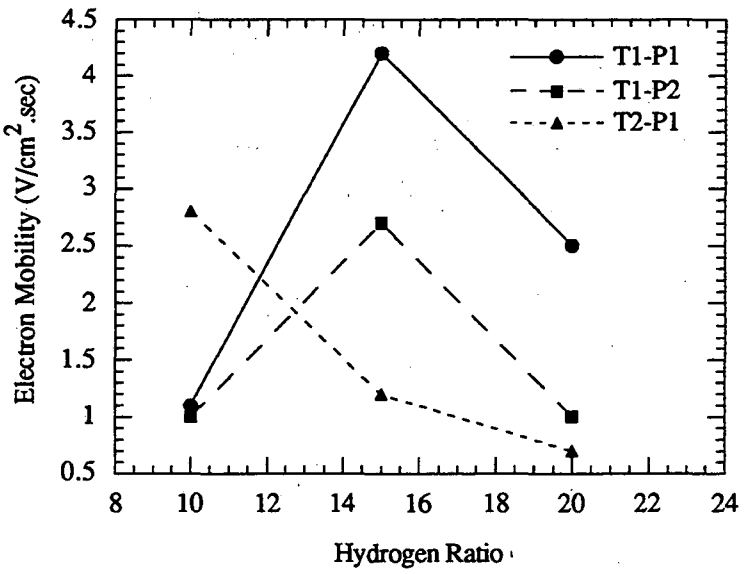

Fig. 2 The effect of hydrogen ratio on electron mobility for 3 different deposition conditions; T1 and T2 refer to T_S of 190 and 250 °C, P1 and P2 refer to RF powers of 60 and 90 mW/cm^2.

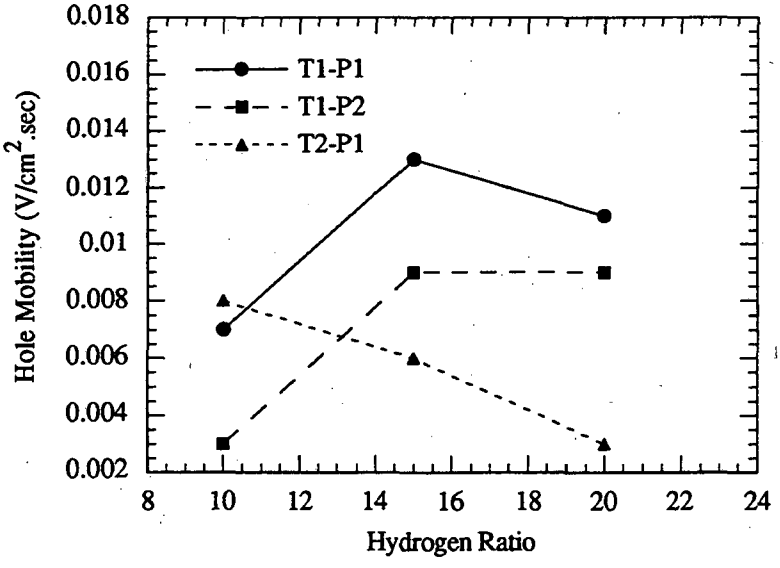

Fig.3 The effect of hydrogen ratio on hole mobility for 3 different deposition conditions; T1 and T2 refer to T_S of 190 and 250 °C, P1 and P2 refer to RF powers of 60 and 90 mW/cm^2.

For the $\mu\tau$ measurements, we used the same experimental setup and measured the collected charges for a set of reversed bias values. The data were then fitted to the Hecht equation[14] in order to derive the $\mu\tau$ values. In Figs. 4 and 5, we show the measured electron and hole μt values as a function of hydrogen ratio. For both electrons and holes, it is apparent that the preferred temperature and power are those of the solid curves (190 °C and 60 mW/cm^2) and the optimum hydrogen ratio is 15. At this deposition condition, the $\mu\tau$ values are about twice the normal a-Si:H values. For the electron $\mu\tau$, the values for higher RF power (dashed lines) samples, show no variation with hydrogen ratio, while for the holes the higher temperature ones show similar behavior.

The density of ionized dangling bonds (N_D^*) was determined by hole onset measurement. In this measurement, the samples were illuminated through the n sides and the signal amplitudes were measured by varying the reversed biases applied to the diodes. The onset voltage found in this manner was assumed to correspond to the full depletion of the device, and was used to calculate N_D^* from eq. (2), where V_a, V_0, and d are: applied reversed bias, built in potential, and detector i layer thickness, respectively.

$$N_D^* = \frac{2(V_a + V_0)\varepsilon_0\varepsilon_r}{qd^2} \qquad (2)$$

The measured values of ionized dandling bond densities for our various samples are given in Fig. 6. The N_D^* values are lowest at a hydrogen ratio of 15, for all three deposition conditions. These values are considerably lower than the value of $7\text{x}10^{14}$ that we normally measure for our standard a-Si:H samples.

We have also measured the I-V characteristics of these hydrogenated samples. The results showed that the reverse currents were about one or two orders of magnitude higher than our best normal a-Si:H diodes. The reverse currents are higher for samples with more hydrogen dilution, and for hydrogen to Silane ratio of 25, some samples had very low forward-to-reverse current ratio. It seems that at this level of hydrogen dilution, the material is no longer free from microscopic defects and the junctions formed at the n and p interfaces do not appear to block the reverse current.

3.2 *Material characteristics*

We used transmission electron microscopy (TEM) images and micro-diffraction patterns to study the microstructure of our samples. X-ray diffraction (XRD) spectra were also used to confirm TEM results. For TEM measurement we deposited ~100 nm thick films on glass

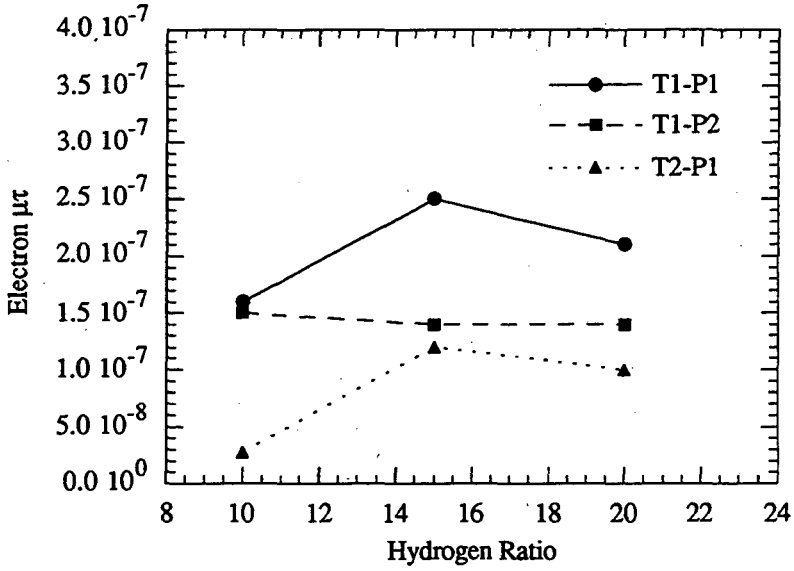

Fig. 4 Variation of electron mt value with hydrogen ratio for 3 different deposition conditions; T1 and T2 refer to T_S of 190 and 250 °C, P1 and P2 refer to RF powers of 60 and 90 mW/cm^2.

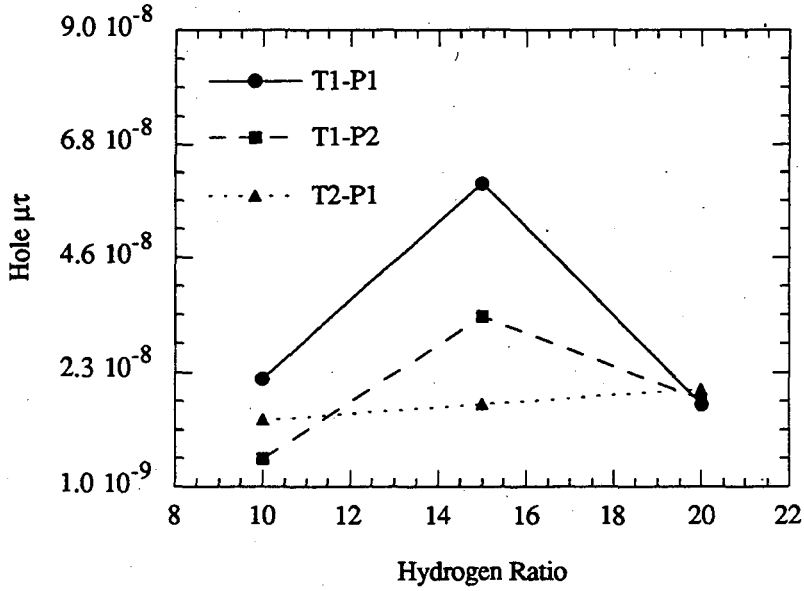

Fig. 5 Variation of hole mt value with hydrogen ratio for 3 different deposition conditions; T1 and T2 refer to T_S of 190 and 250 °C, P1 and P2 refer to RF powers of 60 and 90 mW/cm^2.

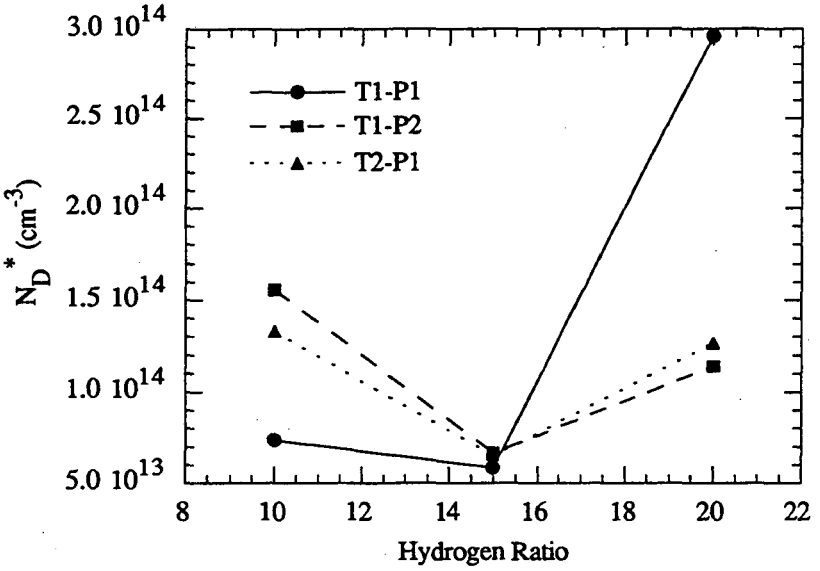

Fig. 6 The effect of hydrogen ratio on the ionized defect density for 3 different deposition conditions; T1 and T2 refer to T_S of 190 and 250 °C, P1 and P2 refer to RF powers of 60 and 90 mW/cm^2.

substrates which were then etched off the glass and used as specimens. For samples deposited with hydrogen ratio greater than 15, both TEM images and micro diffraction patterns showed Si microcrystals embedded in a-Si:H tissue (Fig. 7). The degree of crystallinity and the grain size depend on the deposition conditions. According to our TEM and XRD results, for hydrogen ratio of 20, increasing substrate temperature from 190 °C to 250 °C, increased the crystallinity from 13% to about 23%; whereas, increasing the RF power density from 60 to 90 mW/cm2 decreased it by a factor of about 8. None of these variations affected the grain size drastically, and the average grain size remained about 55 nm. At hydrogen/silane ratio =25, the crystallinity and the grain size were about 20% and 47 nm, respectively. In the XRD spectra of our various samples, a prominent peak at 2θ=47.3 degrees shows that the materials are highly textured with a predominant (220) orientation (see Fig. 8). The same strong (220) orientation has also been reported in ref. 15, for the μc-Si:H films deposited by layer-by-layer technique. For films deposited with hydrogen ratio of 15 or less, neither TEM nor XRD spectra revealed any crystallinity. We used SEM to probe the profile of some of our samples and the results proved that deposited films were indeed free from microscopic defects.

We have also measured intrinsic stress for all of our samples. For stress characterization, we measured the radii of curvatures of the samples and then converted them to stress values from:

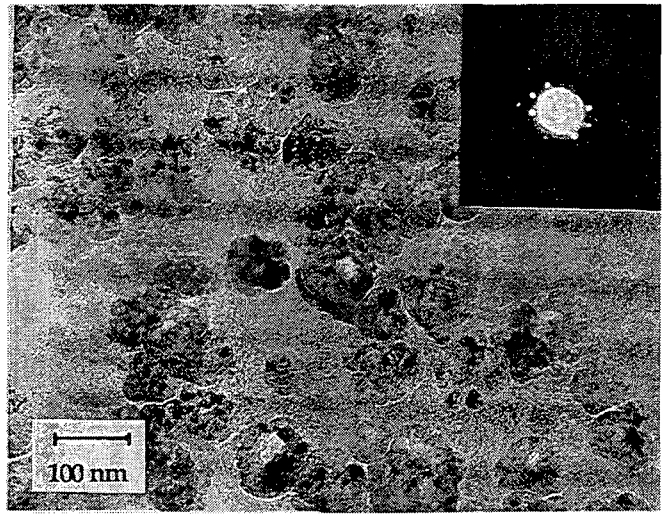

Fig. 7 A TEM micrograph and the associated micro-diffraction pattern for a sample deposited at: H2/SiH4 ratio = 20, Ts = 190°C, and P = 60 mW/cm^2.

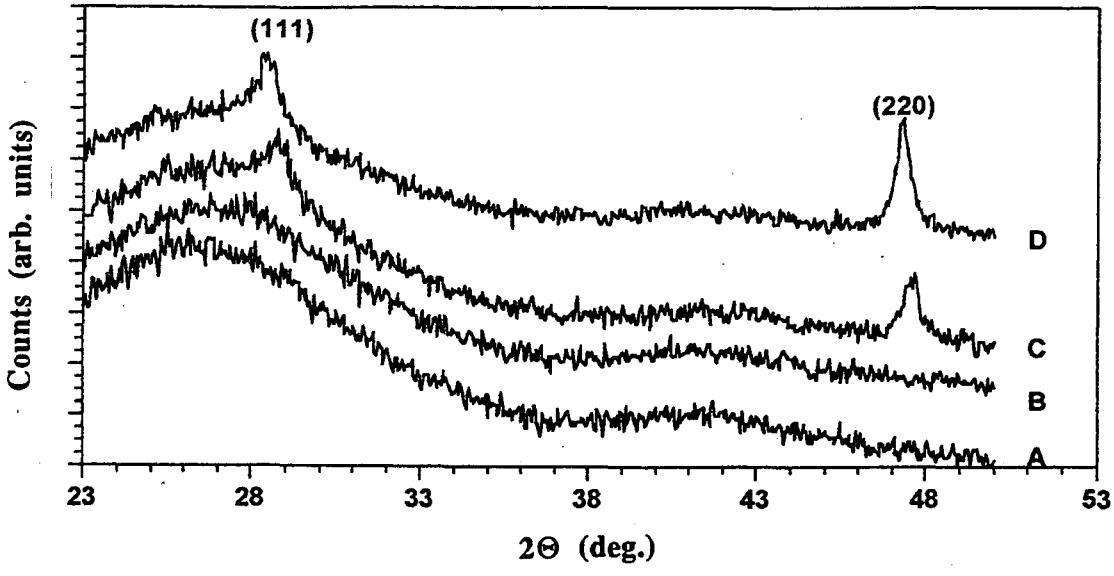

Fig. 8 X-ray diffraction patterns for 4 different deposition conditions. All samples were deposited at T_s = 190°C; for A, B, and D RF power was 60 mW/cm^2 and hydrogen ratios were: 10, 15, and 20, respectively; for C hydrogen ratio and RF power were 20 and 90 mW/cm^2, respectively.

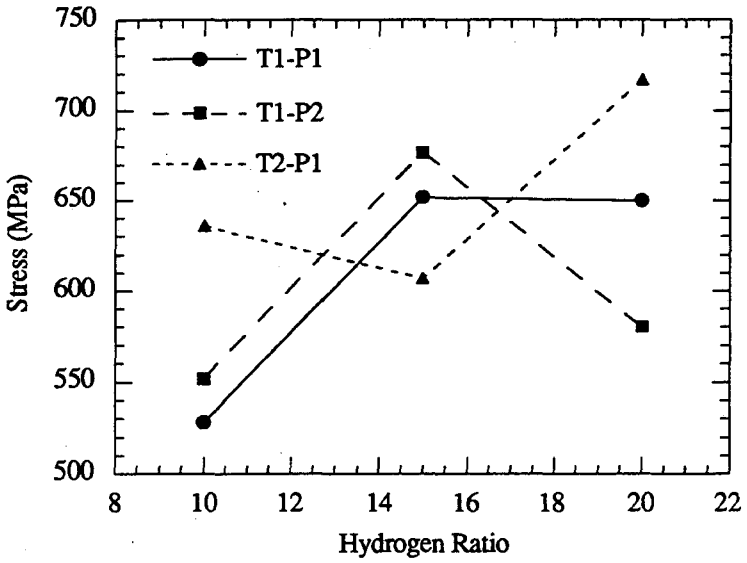

Fig. 9 Variation of intrinsic stress with hydrogen ratio for 3 different deposition conditions; T1 and T2 refer to T_S of 190 and 250 °C, P1 and P2 refer to RF powers of 60 and 90 mW/cm^2.

$$\sigma_t \cong \sigma_i = \frac{E_s t_s^2}{6(1-\nu_s)t_f R} \tag{3}$$

where, E_S, n_S ,and t_S are Young's modulus, Poisson's ratio, and thickness of the glass substrate; t_f and R the film thickness and radius of curvature, respectively. The results of stress measurement for our various samples are shown in Fig. 9. The notations in the legend are explained in section 2 and in the figure caption. The measured stress values are about 1.5 to 2 times that of our standard a-Si:H material.

4. Modeling of microcrystalline effects

As evident in our data and also reported by others, using hydrogen dilution of silane at a certain level, results in production of silicon microcrystals embedded in amorphous material. The presence of microcrystals will affect the electronic transport properties of the material by enhancing the mobility and possibly, decreasing the lifetime of the charge carriers, due to capture by the dangling bonds within the grain boundaries. In the following sections, we will discuss these effects, quantitatively, by applying a simple phenomenological model. In this model, we assume each microcrystal is a sphere with a diameter δ (grain size) surrounded by a grain boundary region of

thickness d. The volume fraction of grain boundaries then would be : $X_b = 6dX_c/\delta$ where X_c denotes the volume fraction of crystallinity.

4.1 *Effects on mobility*

In a mixture of amorphous and microcrystalline phase, average carrier mobility (μ) is related to the mobilities of the amorphous (μ_a), microcrystalline (μ_c) and grain boundaries (μ_b) by:

$$\frac{1}{\mu} = \frac{X_c}{\mu_c} + \frac{X_a}{\mu_a} + \frac{X_b}{\mu_b} \tag{4}$$

where X_a , the volume fraction of amorphous part is approximately equal to 1- X_c . Substituting into eq. (4) for X_a and X_b we obtain:

$$\frac{\mu}{\mu_a} = \frac{1}{1 - X_c(1 - \frac{6d}{\delta}\frac{\mu_a}{\mu_b})} \tag{5}$$

Figure 10 shows a plot of the above ratio as a function of X_c, for three different values of the parameter K defined as: μ_a / μ_b and used in that Fig.'s legend. For the plot we have used a grain size (δ) of 55 nm which is the typical value measured by TEM for our microcrystalline samples, and a value of 0.5 nm for the thickness of grain boundary region. As is seen from the plot, for the volume fraction of crystallinity below ~ 0.25, which is the maximum value we have measured for our samples with hydrogen ratio of 20, the overall mobility would not be noticeably higher than that of the amorphous phase. For higher crystallinity, the model prediction is close to the mobility values for polycrystalline silicon. Meanwhile, the results of this analysis at lower values of volume fraction of crystallinity, are almost independent of the parameter K.

4.2 *Effects on Carriers lifetime*

The average lifetime of carriers in the mixed amorphous-microcrystalline phase (τ) can be defined by:

$$\frac{1}{\tau} = \frac{1}{\tau_a} + \frac{1}{\tau_b} \tag{6}$$

where τ_a and τ_b are lifetimes in the amorphous and grain boundary material, respectively; and the

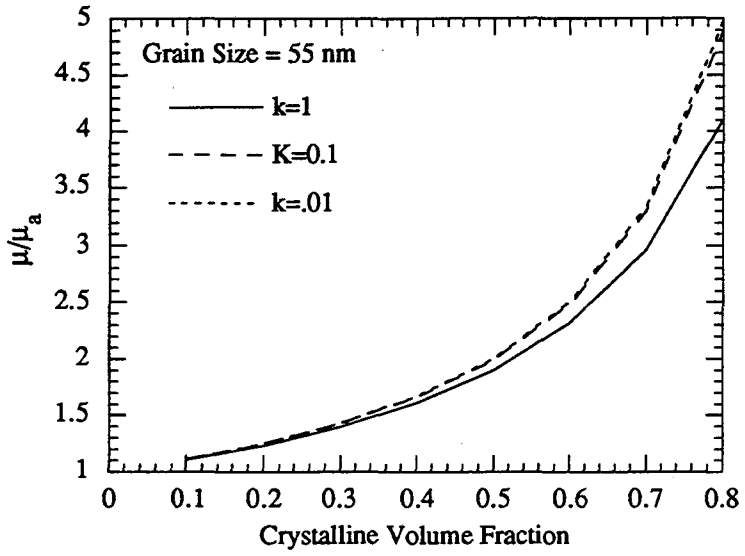

Fig. 10 Results of modeling of the effect of crystallinity variation on the m/m_a ratio for an assumed value of 55 nm for the grain size. The parameter K denotes the ratio of the carrier mobility of the amorphous phase to that of the grain boundary regions.

lifetime in the crystalline part is assumed to be negligibly small. We know τ_a from measurement of our a-Si:H samples, and for our model τ_b can be written as:

$$\tau_b = \frac{\delta}{6vdN_t X_c \sigma} \tag{7}$$

where, v, N_t and σ represent: carrier drift velocity, defect density in the grain boundaries, and capture cross section, respectively. From eq. (6), its obvious that for τ_b much larger than τ_a the life time in the mixture would not be affected by the grain boundaries. Using this criteria, based on eq. (7), one can define regions in the $\delta - X_c$ plane where the effect of grain boundaries on lifetime of either holes or electrons can be neglected ($\tau_b \geq 10\tau_a$). Such regions are shown on Fig. 11 as A and B. In fact, the drawn lines divide the plane into three regions: in region A, both electron and hole lifetimes are unaffected, whereas in B, only electron lifetime, and in C, both electron and hole lifetimes are affected by the grain boundary captures. For this analysis we have assumed the following values for the involved parameters: $v_e = 10^4$ cm/sec, v_b=50 cm/sec, N_t=2x10^{18} cm^{-3}, and σ= 5x10^{-15} cm^2.[16] According to this model, for the material deposited at hydrogen/silane ratio =20, the microcrystalline grain boundaries should not affect the hole lifetimes. For electrons, we may be in region A or B of Fig. 11, depending on which of the TEM or XRD measured grain sizes we use. Anyway, the effect on electron lifetime is not very large either.

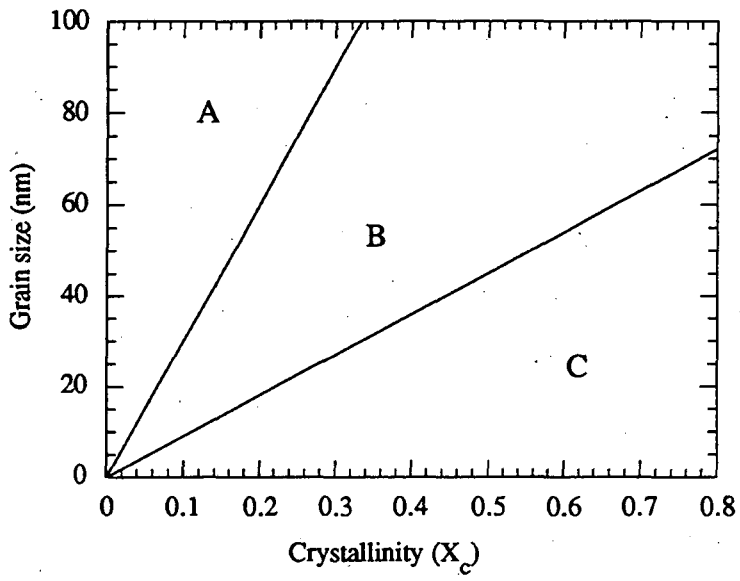

Fig. 11 The effect of crystalline formation on carrier life times. According to our model in region A neither electron nor hole lifetimes are affected by grain boundaries; in B only electron lifetime, and in C both electron and hole lifetimes are affected.

5. Discussion

Based on the measurement results presented in Figs. 2-6, for hydrogen dilution of silane, we have found an optimum deposition condition (hydrogen ratio =15, T_s=190°C, and RF power = 60 mW/cm^2), at which, almost all electronic transport characteristics peak. The electron and hole mobilities are about 3-4 times larger than our standard a-Si:H values. The increase in hole mobilities have also been reported by the Dundee group[12] for their hydrogenated samples deposited by microwave decomposition of H_2 diluted SiF_4. The fact that the increase in crystallinity due to addition of more hydrogen from the level of H_2/SiH_4 =15 or by using higher temperature did not result in any further enhancement in mobilities, but rather caused decrease in their values, leads us to believe that the higher mobilities are not the result of microcrystalline formations. But instead, it is the improvement in the quality of the amorphous material which is responsible for this favorable change. The hydrogen role can then be viewed as diffusing into the growing layers and breaking loose Si-Si bonds and therefore, enhancing the long range order in the amorphous material. This would imply narrower band tails, both at the conduction and the valence mobility edges, which results in higher drift mobilities for both electrons and holes. Even at hydrogen/silane ratio =20, with some 13% crystallinity, both electron and hole mobilities are larger by more than a factor of 2 compared to normal amorphous silicon, while according to our

macroscopic model (see Fig. 10), the presence of microcrystals could hardly improve the mobilities. This further reinforces our argument about improvement of the a-Si:H phase of the material by hydrogen dilution. The higher $\mu\tau$ values for our best sample is primarily due to the increased mobilities and apparently the lifetimes are not changed in a consistent manner, such that one can draw any solid conclusion; but our model prediction of no appreciable effect from grain boundaries for the crystallinity values corresponding to deposition at hydrogen/ silane ratio =20, is consistent with the measured $\mu\tau$ values. The improvement in electrical parameters due to hydrogen dilution have also been reported by other groups.[17-20] They obtained improved photovoltaic characteristics in their amorphous silicon solar cells, using hydrogen dilution, both at initial and light degraded states. It is interesting that our best results are from deposition runs with 190 °C and most of the improved characteristics reported in ref.'s 18-20 are also at low substrate temperatures (80-160 °C). Apparently with hydrogen dilution, the optimum substrate temperature shifts to lower values form the conventional value of 250 °C, used for standard a-Si:H. Therefore, further investigation to explore the substrate temperature range of 100 °C to 190 °C should be considered. Our measured values of ionized defect densities (N_D^*) are lower by a factor of 5-30 than those of normal amorphous silicon samples. The ionized dangling bond density, N_D^* from amorphous silicon samples is $\approx$0.35 of the ESR measured N_D value.[21] Therefore, the lower values of N_D^* for our new samples may mean that, either the defect density in the amorphous part has improved by a large factor, or, for the hydrogen diluted material, the relation between the N_D^* as measured by hole-onset method and the total defect density N_D is different from the one established for standard amorphous silicon. The former may be true, if we assume that the extra hydrogen also plays a role in passivating further some of the dangling bonds in the amorphous part. This is consistent with our stress measurement results which show stress values a factor of 2 higher for our new samples, and the empirically known inverse relation between the internal stress and the dangling bond density .[22]

6. Conclusion

We have obtained an optimum hydrogen dilution of silane for improving the electronic characteristics of a-Si:H deposited in PECVD. For the new hydrogenated samples, we have measured electron and hole μ, $\mu\tau$, and N_D^*. For the optimum deposition condition, we measured mobility values ~3-4 times and $\mu\tau$ values approximately 2 times those of standard a-Si:H. The N_D^* values have also improved. Stress measurements also show higher stress values. At hydrogen to silane gas flow ratio of 20, we start to see microcrystal formations. We have developed a simple model to analyze the effect of microcrystals and their grain boundaries, the results of which are consistent with our measurements. We suggest that these improvements might be due to the hydrogen dilution by postulating the following roles for the extra hydrogen: a) it causes narrowing

the band tails by breaking loose Si-Si bonds and therefore bringing about more long range order; b) passivating some more of the dangling bonds in the amorphous material.

Acknowledgments:

This work was supported by High Energy Physics Division of U.S. Department of Energy under Contract Number DE-AC03-76SF00098. We would like to thank Chalk Etcher of the National Center for Electron Microscopy for preparing some of our TEM images.

References:

1) A. Matsuda: *Amorphous Semiconductor Technologies and Devices,* ed. Y. Hamakawa (OHMSHA and North Holand, 1987) JARECT 22, pp. 111-119.
2) Y. Uchida, T. Ichimura, M. Ueno and H. Heruki: Jpn. J. Appl. Phys. 21 (1982) L 586.
3) Y. Matsumoto, G. Hirata, H. Tkakura, H. Okamoto and Y. Hamakawa: J. Appl. Phys. 67, (1990) p. 6536.
4) L. Yang, L. Chen, S. Wiedeman and A. Catalano: Mat. Res. Soc. Symp. Proc. 283 (1993) p. 463.
5) S. S. He, M. J. Williams, D. J. Stephens and G. Lucovsky: J. Non-Cryst. Solids 164-166 (1993) p. 1263.
6) V. Perez-Mendez, J. Morel, S. N. Kaplan and R. A. Street: Nucl. Instrum. & Methods A252 (1987) p. 478.
7) V. Perez-Mendez: *Amorphous and Microcrystalline Semiconductor Devices,* ed. J. Kanicki (Artech House, Boston, 1991) pp. 297-330.
8) A. Mireshghi, G. Cho, J. Drewery, T. Jing, S. N. Kaplan, V. Perez-Mendez and D. Wildermuth: IEEE Trans. Nuc. Sci. NS-39 (1992) p. 635.
9) B. Equer and A. Karar: Nucl. Instrum. & Methods A275 (1989) pp. 558-563.
10) Y. Mishima, S. Miyazaki, M. Hirose and Y. Osaka: Philos. Mag. B 46 (1982) p. 31.
11) K. P. Chik , P. H. Chan, B. Y. Tong, S. K. Wong and P. K. John: Philos. Mag. B 61 (1990) p. 377.
12) A. C. Hourd, D. L. Melville and W. E. Spear: Philos. Mag. B 64 (1991) p. 533.
13) A. Mireshghi, W. S. Hong, J. Drewery, T. Jing, S. N. Kaplan, H. K. Lee and V. Perez-Mendez: to be published in Mat. Res. Soc. Symp. Proc. (1994).
14) R. A. Street: Phys. Rev. B 27 (1983) p. 4924.
15) S. Ishihari, Deyan HE, T. Akasaka, Y. Araki, M. Nakata and I. Shimizu: Mat. Res. Soc. Symp. Proc. 283 (1993) p. 489.
16) R. A. Street: *Hydrogenated Amorphous Silicon,* eds. R. W. Cahn, E. A. Davis and I. M. Ward (Cambridge University Press, Cambridge, 1991) p. 314.

17) P. K. Acharya, H. D. Banerjee, K. L. Chopra, S. C. Saha and Swati Ray: Sol. Energy Mater. & Sol. Cells 32 (1994) pp. 21-28.
18) Y. Hishikawa, S. Tsuge, N. Nakamura, S. Tsuda, S. Nakano and Y. kuwano: J. Appl. Phys. 69 (1991) No. 1, p. 508.
19) Y. Hishikawa, M. Sasaki, S. Tsuge, S. Okamoto and S. Tsuda: Mat. Res. Soc. Symp. Proc. 297 (1993) p. 779.
20) J. Yang, X. Xu and S. Guha: to be published in Mat. Res. Soc. Symp. Proc. (1994).
21) S. Qureshi, V. Perez-Mendez, S. N. Kaplan, I. Fujieda, G. Cho and R. A. Street: IEEE Trans. Nucl. Sci. NS-36 (1989) p 194.
22) W. E. Spear and M. Heintze: Philos. Mag. B 54 (1986) p. 343..

LAWRENCE BERKELEY LABORATORY
UNIVERSITY OF CALIFORNIA
TECHNICAL INFORMATION DEPARTMENT
BERKELEY, CALIFORNIA 94720